The Infrared Spectrum of Ozone from 0.6 to 2.8 Microns

Final Ch 80 Report

Alan C. Wright

Advisor: Dr. Richard M. Badger

California Institute of Technology
May, 1963

The Infrared Spectrum of Ozone from 0.6 to 2.8 Microns

Abstract: The spectrum of ozone from 0.6 to 2.8 microns has been investigated under medium dispersion. By use of a multiple pass cell an equivalent path of 60 cm ozone was achieved with a 2.5% concentration of ozone in oxygen.

Eleven new overtone and combination bands of the ground state molecule were observed in the range 3700 to 5000 cm^{-1}. Using these bands along with previously reported fundamental and lower overtone and combination bands, the three linear and six quadratic constants in the vibrational energy expression are calculated, leaving nine bands to check the band assignments and calculated constants. The linear constants are then used to calculate the two potential constants of ozone assuming a valence force field. The third independent equation checks satisfactorily, indicating the adequacy of the valence force field for ozone.

In the region 0.6 to 1.1 microns, the Wulf vibronic bands were investigated. Rather surprisingly, one band at the red end of the series shows structure. A partial analysis of this band and a consideration of other factors offer evidence that the Wulf bands arise from a transition between two excited states. In particular, a $^1A_2 \leftarrow A\,^1B_1$ transition is proposed. The weak Chalonge-Lefebvre system at 3440 A is tentatively identified as the forbidden $^1A_2 \leftarrow X\,^1A_1$. Several objections, one perhaps fatal, are given to the proposed transition.*

The spectrum of ozone in the region 0.6 to 2.8 microns contains two observed types of transitions. The first is an electronic transition which gives rise to a weak series of vibronic bands in the range 0.6 to 1.1 microns. At longer wavelengths the overtone and combination bands of the ground state vibrations are observed. Accordingly this paper is presented in two sections, the first part dealing with the vibrational spectrum, the latter with the vibronic band series.

I. The Vibrational Spectrum

I.A. Introduction

Infrared and microwave studies have firmly established that the ground state ozone molecule belongs to the symmetry group C_{2v}. A drawing of the three normal vibrations, all infrared active, is shown in Fig. I. The fact that two of the fundamental bands, ν_1 and ν_3, somewhat overlap and are of greatly dif-

---

*See Appendix (added June, 1963).

ferent intensities led to an initial assignment of fundamentals which overlooked the weaker band.[1] This early assignment required the apex angle of the ozone molecule to be acute. A dissatisfaction with this acute-angled model, due to the rather unlikely interatomic distances involved, prompted Wilson and Badger[2] to reinvestigate the far infrared spectrum and, as a result, to suggest that the ν_1 band is masked by the much stronger ν_3 band. Their new assignment, given in Fig. I, leads to the presently accepted obtuse-angled model. Subsequent microwave measurements[3] and analyses of the fundamental vibrational transitions[3,4] have borne out the assignment of Wilson and Badger.

The present investigation of the near infrared yielded ten additional overtone and combination bands whose frequencies can be fitted without difficulty to the scheme of Wilson and Badger. By using five of these bands frequencies along with values for the fundamental and lower overtone and combination bands, the three linear and six quartic vibrational energy constants have been calculated, leaving nine other bands to check the validity of the band assignments and calculated constants. These results are presented in Table I.

I.B. Theoretical Considerations

For a thorough treatment of the non-linear symmetrical AB_2 molecule, the reader is referred to Herberg[5]. Only a brief resumé of the properties which are pertinent to this investigation can be given here.

The vibrational energies which the ozone molecule may assume in the absence of perturbations are given by the formula

$$G(v_1, v_2, v_3) = \sum_{i=1}^{3} \omega_i (v_i + 1/2) + \sum_{i \le j}^{3} x_{ij} (v_i + 1/2)(v_j + 1/2) + \ldots ; \quad v_k = 0, 1, 2, \ldots \qquad (1)$$

where all terms other than those involving the ω_i arise from anhormonicities, and where v_k gives the degree of excitation of the kth normal mode. To the

(Note: Footnotes are given at very end of paper)

approximation that the normal vibrations are harmonic and that the variable dipole moment is a linear function of the normal coordinates, we have the selection rule $\sum_i \Delta v_i = 1$ for electric dipole transitions; i.e., only the fundamentals may be observed in transitions to the ground level. However, since these approximations always fail to some extent, comparatively weak overtone and combination transitions are observed for sufficiently great absorbing layers.

The three normal vibrations of the ozone molecule fall into two symmetry types, classified by whether the nuclear displacements are symmetric (species A) or antisymmetric (species B) to a two-fold rotation about the C_2 axis of the non-vibrating molecule. Thus, as shown in Fig. I, ν_1 and ν_2 are of species A, while ν_3 is of species B. The foregoing is, of course, equivalent to saying that the vibrational wavefunction $\psi(v_1, v_2, v_3)$ is of species A for $(1,0,0)$ and $(0,1,0)$, and of species B for $(0,0,1)$. More detailed study shows that all ψ involving odd v_3 are of species B, while those wavefunctions involving even v_3 are of species A. Accordingly all vibrational transitions to the ground level are of species A or B depending upon whether v_3 in the upper level is even or odd respectively.

A consideration of the different electronic configurations which are likely to contribute to the ground electronic state of ozone shows that the end atoms each carry a negative charge and the apex atom a positive charge.[6] This charge distribution, shown is Fig. II, results in a permanent electric dipole moment aligned along the symmetry axis. Since the dipole moment undergoes a change for each of the normal vibrations, all the fundamentals are active in the infrared. In accordance with group theory expectations, the change in the dipole moment associated with ν_1 and ν_2 is of species A, being along the symmetry axis. The species B dipole moment variation for ν_3 has its major component perpendicular to the symmetry axis.

Detailed consideration[5] of the allowed rotational transitions occurring along with the vibrational transitions to the ground level show that the bands have a $\perp$ or $\parallel$ appearance depending on whether the upper state is of species A or B respectively. These observations assume that the ozone molecule is approximately a symmetric top and that the rotational constants for the excited vibrational levels are not greatly different from those of the ground level.

Experimentally we find that even the ν_3 fundamental band does not display a well-developed Q branch because of the difference in the rotational constants of the two levels involved.[4] Since this difference will in general be even larger for the overtone and combination bands, one would not expect to observe prominent Q branches in these bands. Another consequence of the difference in rotational constants is degradation of the bands to the red, and in the case of higher overtone and combination bands, the development of band heads on the violet side even at room temperature.

The fact that the ν_3 band is much more intense that either the ν_1 or ν_2 band indicates that transitions involving the component of the dipole moment perpendicular to the symmetry axis should be more intense than those transitions which do not. Or equivalently, those transitions to the ground level for which ν_3 in the upper state is odd should be more intense than those for which ν_3 is even. This indication is confirmed in that all of the lower overtone and combination bands so far observed involve odd ν_3. Consequently it has been assumed that all bands found in the present investigation also involve only odd ν_3 in the upper level. No difficulty seems to be encountered because of this assumption.

I.C. Experimental

The high resolution vacuum spectrophotometer located in the Crellin Building at the California Institute of Technology was used in the investigation. The grating employed has 7500 lines per inch, a ruled surface of 5 by 6 inches, and is blazed for about 3.5 microns in the first order. A CO_2 cooled dewar-type PbS detector having rated detectivity $D^*(500, 1000, 1) \geq 4 \times 10^9$ cm/watt (-78°C), maximum noise-equivalent-power at about 2.7 microns, and a sensitive area of 2x3 mm was used. Very approximate calculations indicate that for some unknown reason the actual detectivity was about 100 times less than the figure given above. A 500 watt tungsten lamp driven at 130 volts from a regulated supply served as the radiation source. The amplifier employed has a maximum amplification factor of 2×10^7, with a band width of about 3 cycle/second (760 cycle/second signal) at maximum amplification. It was found that the limiting factor in the signal-to-noise ratio lay in the detector rather than the amplifier. A Brown chart recorder was used. Figure III schematically shows that entire experimental apparatus, giving important dimensions.

Wave length calibration was accomplished by using Hg emission and H_2O absorptions lines. Absolute wavelengths are estimated to be accurate to within three Angstroms. From observations of the H_2O band at 1.9 microns, it was found that the observed resolution at various slit widths agreed well with the theoretically calculated resolution. Since a variety of slit widths were employed in observing the bands, the theoretical resolutions are marked on each tracing (Figs. IV-IX). Resolution was limited by the signal strength rather than the optics of the system.

The ozone was produced by two water-cooled (8°C) Berthelot ozone generators connected in parallel. Dryed oxygen (>98% pure) was fed into the generators at a measured rate of flow. The ozone concentration of the output mixture, as measured by iodometric methods, was about 3.4% by volume at the rate

of flow which maximized the White (multiple pass) cell ozone content. The oxygen-ozone mixture was passed through two CO_2 cold traps before being admitted to the White cell to eliminate any of the heavier nitrogen oxides. In one run, about 5% nitrogen was purposely added to the oxygen flowing into the generators. No new bands or changes in intensity in the old bands were noted. The only impurities detected spectroscopically were water vapor, small amounts of CO_2, and traces of formaldehyde. The latter two impurities are believed to be the result of ozone attack on plastic tubing and stopcock grease present in the system. Since neither impurity proved to be present in troublesome quantities, glass tubing was not substituted.

The White cell employed is constructed of aluminum wherever possible because of the relatively high resistance of aluminum to ozone attack once a thin oxide layer is formed. The cell has a volume of about 30 liters and is one meter in length. Gold surfaced mirrors were used in the cell to take advantage of the high reflectivity of gold in the near infrared. In the wavelength region of interest up to 28 meters of path were easily attained, the intensity loss at 28 meters being about 65%.

The oxygen-ozone mixture was admitted continuously to the White cell during the course of each run. The average cell ozone concentration was determined before and after each run by the amount of absorption in the Chappuis band of ozone centered at 0.6 microns[18]. The estimated accuracy of these determinations is ±0.2% ozone concentration. Equivalent paths (STP) for each run are noted on the individual charts. All runs were made at room temperature.

I.D. Observations and Vibrational Assignments

Tracings of the eleven bands observed in this study are shown in Figures IV-VIII. Immediately below each band tracing is a background tracing taken in the absence of ozone. As can be seen, the two longest wavelength bands are very badly obscured by the 2.8 micron water vapor band (CO_2 is also quite

evident in the longest wavelength tracing). Sketches of the general shapes of these two bands, suggested by careful comparison with background tracings, are drawn in. Fig.IX is a fairly high resolution tracing of the particularly strong band at 4025 cm^{-1} which partially resolves the rotational structure. No rotational analysis of this band was attempted.

All of the bands show strong head development on the violet side. In some cases the band head is the only feature observable. The choice of band origins noted on the tracings is of course largely a matter of guesswork. For lack of a better criteria, the amount of head development was considered in a rather subjective way in choosing origins.

The small absorption peak at the red side of the 4517 cm^{-1} band (Fig. V) was first thought to be due to ozone. Subsequent attempts to make an assignment for this peak resulted in energy constants which failed to adequately represent the remaining data. Upon investigation of possible impurities which might accompany ozone, it was discovered that the peak occurs at the wavelength (2.18 microns) given by Salent and West[7] for one of the stronger bands of formaldehyde. Further evidence for this identification is given by Trambarulo, Ghosh, Burrus, and Gordy,[10] who detected formaldehyde, apparently formed by the attack of ozone on stop-cock grease, during their investigation of ozone in the microwave region.

Table I presents the band center energies, assignments, and peak extinctions of all the bands noted in this study along with similar data for the fundamental and lower overtone and combination bands. The starred bands were used in determining values for the ω_i and x_{ij} (also given in Table I) in the vibrational energy expression (Eq.(1)). Using these constants the energies of the remaining nine bands were calculated. Considering the uncertainties in locating the band origins as well as the approximate nature of the vibrational energy expression employed (i.e., no terms higher than quadratic), the agree-

ment between ν_{cal} and ν_{obs} seems satisfactory. Since the value of 1740 cm^{-1} for the (0,1,1) band was taken from early low dispersion tracings, it is quite possible that the disagreement between ν_{cal} and ν_{obs} is more apparent than real.[8] In the case of the (0,0,5) band, the positive, relatively large difference is probably due to the absence of higher terms in the vibrational energy expression used here.

Perturbation between the (2,2,1) and (0,5,1) levels is indicated both by their respective deviations from ν_{cal} and by their near equality in intensity. Assuming that one may still meaningfully speak of unmixed states, it may well be the case that the assignment should be the reverse of that given in Table I. The (3,1,1) and (0,0,5) levels are also likely perturbed to some extent. Since perturbation between levels of different species do not occur[5], no concern over the species A levels which are calculated to lie in the wavelength range of this investigation need be taken.

I.D. Recalculation of Force Constants.

Various approximate potential functions have been used to describe the interatomic forces of the non-linear symmetric AB_2 molecule. The simplest of these assume that the forces are proportional either to the interatomic distances (central forces) or to the degree of bond stretching and bending (valence forces). Empirically the valence force field has proved to be much superior to the central force field in the case of AB_2 molecules.

In either case, since the potential functions are assumed to be quadratic, the ω_i (i.e., the normal frequencies for infinitesimal displacements) should be used in solving for the various constants. However, in practice, the observed fundamental frequencies ν_i, which are affected by anhormonicities, are often used whenever the ω_i cannot be determined from existing data. The

additional bands noted in this investigation have furnished the necessary data to determine the ω_i for ozone, and, hence, a recalculation of the force constants is worthwhile.[9]

Assuming valence forces, the potential function for ozone has the form $2V = k_r(\Omega_1^2 + \Omega_2^2) + k_\alpha \delta^2$

where Ω_1 and Ω_2 are the displacements along the bonds and δ is the change in the apex angle. If we let $x = \frac{k_r}{4\pi^2 m c^2}$

$$y = \frac{k_\alpha}{4\pi^2 m c^2 r_0^2}$$

then the equations relating the normal frequencies to the force constants have the simple form $\omega_2^2 \omega_1^2 = 6xy$ (i)

$$\omega_3^2 = (1 + 2\sin^2\alpha)x \quad \text{(ii)}$$

$$\omega_1^2 + \omega_2^2 = (1 + 2\cos^2\alpha)x + 2(1 + 2\sin^2\alpha)y \quad \text{(iii)}$$

where r_0 is the O-O bond distance and 2α is the magnitude of the apex angle for the nonvibrating molecule.[5]

Using the value $2\alpha = 116\ 49'$ determined from microwave studies[6] and the values for the ω_i given in Table I, we calculate from Eqs.(i) and (ii) that $x = 0.49339 \times 10^6$ cm^{-2} $\Rightarrow$ $k_r = 4.64_{84} \times 10^5$ ergs cm^{-2}

$y = 0.21318$ " $k_\alpha/r_0^2 = 2.00_{84} \times$ "

The adequacy of the valence force field in describing the internuclear forces for ozone is demonstrated by using Eq.(iii) as a check. From the above values of x and y, the right hand side of Eq.(iii) is calculated to be 1.8093×10^6 while the left hand side is 1.8003×10^6 cm^{-2}. Use of a central force field leads to a much less satisfactory check.

II. The Wulf Vibronic Band Series

II. A. Introduction

The vibronic bands studied in this investigation were first noted in 1930 by O.R. Wulf[11], who represented the band energies by the simple formula

$$\nu(cm^{-1}) = 10,000 + 566.7\,n\,, \quad n = 0, 1, \ldots, 9. \qquad (2)$$

As his photographs show, the bands are weak and present a diffuse appearence. Underlying both the Wulf bands and the higher-lying Chappuis bands is a region of continuous absorption which peaks at about 0.6 microns and falls off steadily on either side (shown in Fig. X)

In 1935, L. Lefebvre[12] reinvestigated the region of the Wulf Bands and gave six additional lines, all of which roughly cluster about those reported by Wulf.

An assignment of the transition which gives rise to the Wulf bands is still undecided. Mulliken[16], in his tentative assignments for the electronic spectra of ozone (given in Table III), has assumed that the Wulf bands either arise from an impurity, perhaps O_4, or from a transition between excited states. G.W. Robinson[13] has suggested that the forbidden $a^3B_1 \leftarrow X^1A_1$ is their source.

It was hoped that the present study, through the use of higher resolution than has previously been employed, would reveal the multiplicity of the transition responsible for the Wulf bands. Unfortunately experimental limitations prevented the attaining of resolutions better than about 15 cm^{-1} in the region of the most intense bands. Nevertheless, the results of this study point to the correctness of Mulliken's second proposal, that the Wulf bands arise from a transition between two excited states. It should, however, be emphasized that there are objections, perhaps fatal, to this proposal. A simple experiment, outlined in the last section of this paper, should suffice to support or disprove the specific proposal to be set forth.

II. B. Theoretical Considerations

The electronic states of light AB_2-type molecules have been the subject of extensive experimental and theoretical interest for about 25 years. To the present, one of the most fruitful theoretical approaches has been the calculation of molecular orbital energies as a function of the apex angle α[14,15,16]. These calculations have met with considerable success in explaining the equilibrium nuclear configurations in excited states as well as gross features of electronic spectra.

The qualitative characteristics of these orbital energy calculations are displayed in Fig.XI, a so-called "Walsh diagram"[15] for a general AB_2 molecule composed of light atoms. The Walsh diagram should not be regarded as being any more than very roughly quantitative, since it neglects the affects of electron correlation and also wrongly predicts identical energies for all the possible states of a given configuration.

The reader is referred to Mulliken[16] for the theoretical representation of the various molecular orbitals. The convention used in naming the orbitals in the bent case is to give the species (C_{2v}) of the orbital as a small letter which is preceded by an integer denoting the orbital's energy order among all the orbitals of the same species. Thus, for example, $3b_1$ is the third lowest lying orbital which transforms as B_1. The electronic states are also named according to their transformation properties (given by the direct product of the orbital species). Thus $^1A_1$ denotes a singlet (superscript) state whose wavefunction is of species A_1. In classifying the various properties relating to a AB_2 molecule, the atoms are taken to lie in the yz-plane with the z-axis along the C_2 axis. For an excellent discussion of the role of symmetry in electronic states, see Sponer and Teller's "Electronic Spectra of Polyatomic Molecules."[17]

In order that a transition be allowed (to a first approximation) be-

tween two states, the product of the electronic parts of the two wavefunctions involved must have the species of a translational mode.[17] The component of the dipole moment involved in the transition is given by the direction of the translation. As noted in Part I, we would predict transitions involving the dipole moment along the y-axis to be strongest, along the z-axis to be of intermediate intensity, and along the x-axis, weakest. The selection rules for ozone are summarized in Table II.

Despite this fairly well developed theoretical framework, the assignment of the observed electronic spectra of ozone is at this time still tentative. In the discussion of experimental results, I follow Mulliken's assignments, given in Table III.

II. C. Experimental

The experimental setup for this portion of the spectrum was the same as for the longer wavelength portion (described on pp.6-7), with the exception that long wavelength cut-off filters were employed to reduce the stray light intensity. Because of variations in the grating efficiency as well as difficulties in finding adequate filters, it was found that the higher orders offered no advantage over the first order spectrum. Hence the first order was used.

Both the detector response and the reflectivity of the White cell mirrors fell off towards shorter wavelengths. Thus the path lengths and slit widths concomitant with a good signal-to-noise ratio varied from 28 m and 0.15 mm (2.5 cm^{-1}) at 1.2 microns to 16 m and 0.30mm (25cm^{-1}) at 0.6 microns. A further factor inducing an intensity loss at shorter wavelengths is the continuous absorption underlying the Wulf bands (see Fig.X).

II. D. Observations and Discussion of Results

All of the bands with the exception of one showed no sort of prominent structure. A typical tracing of the strongest bands is shown in Fig.XII. As well as could be judged, the weaker bands, except one to be discussed below, displayed the same form as those shown in Fig.XII. This judgement, however, must be regarded as tentative. Determination of the band shapes and wavelengths of maximum absorption is complicated both by the rather rapid changes of grating efficiency in this region as well as by the underlying continuous absorption which limits the usefulness of background tracings taken in the absence of ozone. To minimize the former source of error both "sides" of the grating (i.e., both positive and negative angles of rotation from the zero-angle position) were used, since the respective variations in efficiency are different.

Table IV presents the results of several independent measurements of the band maximums to show the scatter of values. Also given in Table IV are the average values of the wavelengths measured, their respective energies, the resolution employed in observing each band, and the estimated maximum extinctions above the continuum. A least square curve involving both linear and quadratic terms was fitted to the average energies with the result

$$\nu(cm^{-1}) = 9528.4 + 533.61\,x + 2.654\,x^2 \qquad x = 0, 1, \ldots, 10.$$

ν_{cal} and ν_{obs} are compared in Table IV.

The band maximums observed agree closely with those reported by Wulf. The one band found further to the red without question belongs to the same series (i.e., $x=-1$ in Wulf's formula, Eq.(2)). The six additional lines found by Lefebvre were not evident. All of them, however, would fall on some region of the band absorptions noted here. It should be mentioned that in both Wulf's case and the present one, about 3% ozone was present in the absorption path as opposed to about 20% in Lefebvre's case. In all three studies the equivalent paths were roughly equal.

While in conversation with Dr. Wulf, he expressed surprise at the weakness of the bands as observed in this study. Even making generous allowance for our different experimental setups and modes of observation, Dr. Wulf estimated that the bands were likely more than twice as intense in his study as in the present one. This observation alone may be subject to reasonable doubt due to the difficulty of measuring relative transmission from photographic plates. Several other factors to be explained below, however, offer confirmation of this intensity difference.

The one band which shows structure occurs at 0.992 microns, the next to the last band on the red end of the series. The last band was too weak to determine anything more than its mere presence. Besides displaying a prominent head on the violet side, the 0.992 micron band has small but fairly reproducible peaks of absorption on the main band body. A typical tracing is shown in Fig.XIII. Below Fig.XIII is a table of the lines which seemed reproducible. (Six tracings were compared. The lines given appeared on four or more of them.) Most of the lines are adequately represented by the formula

$$\nu(cm^{-1}) = \nu_{head} - 10 - 1.210(x+2)^2 \qquad x = 1, 2, \ldots, 11 \qquad (3)$$

ν_{obs} and ν_{calc} are compared in the table below Fig.XIII.

Both the magnitude of the quadratic term constant and the total number of lines implied to be present (i.e., 2+11) suggest that the peaks are some sort of sub-branch structure. That only one set of peaks seems to be present implies the band is $\parallel$, though it is quite possible that were the band $\perp$, the returning sub-branches ($\Delta K = +1$) might roughly coincide with the peaks for $\Delta K = -1$. (The drawings prepared by N. Metropolis[19] are especially helpful in considering the various band structures possible for electronic transitions.) The above conclusions can only be regarded as tentative, however, due to the very low intensity of the peaks present, poor resolution, and a noise level comparable to the absorption being observed.

Regardless of the tentativeness of the conclusions regarding the fine structure, we may safely comment on the general band shape. The absence of a sharp band head strongly suggests that the K structure and J structure degrade in opposite directions. Since for even fairly large changes in apex angle the K structure of ozone is about five times as coarse as the J structure, the K structure must degrade to the red while the J structure degrades to the violet (Metropolis's[19] Case II).

In considering the implications of these observations, we must also discuss the total band series appearance. The presence of only one series of bands indicates that only one molecular parameter, i.e., either the apex angle or the O-O bond distance, undergoes an appreciable change during the transition. Since the series is long and has its most intense members well to the violet of the lowest energy band observed, the parameter involved must change considerably. As only one parameter is involved we may directly apply Metropolis's Case II and conclude that the apex angle is smaller in the upper state. Thus the Wulf bands are almost certainly a ν_2 series. This is also suggested by the small divergence rather than convergence of the band energies.

We now turn to a discussion of the electronic transition involved. Ozone in its ground state is represented by

$$K(18)(1a_2)^2(3b_2)^2(4a_1)^2;\ {}^1A_1 \equiv \underline{X}\,{}^1A_1$$

where $K(18)$ denotes the orbital product of all but the upper six electrons (see Walsh diagram, Fig. XI). It should be stated that there is some uncertainty regarding the energy ordering of the $1a_2$, $3b_2$, and $4a_1$ orbitals. The transitions tentatively identified by Mulliken (Table III) are thus

$$\underline{A}\,{}^1B_1 \equiv K(18)(1a_2)^2(3b_2)^2(4a_1)(2b_1);\ {}^1B_1 \leftarrow \underline{X}\,{}^1A_1 \qquad E_{vert} = 2.04 \text{ ev}$$

$$\underline{B}\,{}^1B_2 \equiv K(18)(1a_2)(3b_2)^2(4a_1)^2(2b_1);\ {}^1B_2 \leftarrow \underline{X}\,{}^1A_1 \qquad E_{vert} = 4.85 \text{ ev}$$

A glance at the Walsh diagram suffices to show that the transition most likely to cause a large decrease in apex angle is a transition to $4a_1$. Since this is not possible for $O_3(X\,^1A_1)$ because $4a_1$ is filled, the most probable alternative is

$$K(18)(1a_2)^2(3b_2)(4a_1)^2(2b_1);\,^1A_2 \leftarrow K(18)(1a_2)^2(3b_2)^2(4a_1)(2b_1);\,^1B_1 \qquad E_{vert} = 1.55\ ev$$

i.e., an electron jump from $3b_2$ to the half-filled $4a_1$ in $O_3(A\,^1B_1)$.

This assignment is suggested by several factors. (1) A transition between excited states is suggested by Dr. Wulf's observations on the band intensities (p.15). The lesser intensity observed in this study can be explained by the rapid cut-off of the White cell mirrors at wavelengths shorter than about 6500A. In Wulf's study a straight 33m absorption column was employed along with a carbon arc source. Thus it is not unreasonable to believe that the average density of $O_3(A\,^1B_1)$ was greater during Wulf's experiment than during the present one. (2) A transition between the two relatively non-bonding orbitals,[16] $3b_2$ and $4a_1$, would not likely effect the O-O bond distance appreciably. (3) $4a_1 \leftrightarrow 3b_2$ is predicted to be a strong transition, while predictions for other possible orbital transitions (single electron) are:

$4a_1 \leftrightarrow 1a_2$	Species A_2; forbidden
$3b_2 \leftrightarrow 1a_2$	B_1; weak
$2b_1 \leftrightarrow 4a_1$	B_1; weak
$2b_1 \leftrightarrow 3b_2$	A_2; forbidden (See Table II)

(4) The transition gives rise to 11 bands, in agreement with the tentative analysis of the 0.992 micron band.

If we make some reasonable assumptions concerning the internuclear distances in $O_3(A\,^1B_1)$ and also assume that the O-O bond distance undergoes no change during the proposed $^1A_2 \leftarrow A\,^1B_1$ transition, then we may use Eq.(3) to calculate the apex angle α' in $O_3(^1A_2)$. From Eq.(3) we have[19]

$$[A' - \tfrac{1}{2}(B'+C')] - [A'' - \tfrac{1}{2}(B''+C'')] = -1.210\ cm^{-1}$$

From the observed band intensities in the $\tilde{A}\,^1B_1 \leftarrow \tilde{X}\,^1A_1$ transition and the use of a stretching force constant slightly smaller than that for the ground state ($k_r'' = 4.6\times10^{-11}$ ergs A^{-2}), I estimate

$$\alpha'' \approx 120^\circ \ (?) \qquad \text{(change from } \alpha \text{ in } O_3(\tilde{X}\,^1A_1) \text{ is small)}$$
$$r_e'' \approx 1.32\ \text{Å}$$

Solving Eq.(4) by graphical means, assuming that $r_e' = r_e''$, we find that $\alpha' = 105^\circ$, a not unreasonable result. Naturally this result is decidedly tentative.

Fig.XIV is a diagram showing the approximate state energies implied by this analysis. The ν_2 potential wells are merely schematic, showing the likely relative equilibrium apex angles and estimated degree of ν_2 excitation for the various transitions. The figure suggests that we identify the weak Chalonge-Lefebvre band system with the forbidden $^1A_2 \leftarrow \tilde{X}\,^1A_1$ transition. The observed energy of this transition is about 3.58 ev (Table III), which is almost exactly equal to the sum of the energies of the $\tilde{A}\,^1B_1 \leftarrow \tilde{X}\,^1A_1$ and proposed $^1A_2 \leftarrow \tilde{A}\,^1B_1$ transitions.

A survey of the lines reported by Chalonge and Lefebvre[20] shows a good number of 500-560 cm^{-1} intervals between lines. However, no exhaustive analysis was attempted and there are many lines within a relatively small spectral interval. Therefore, these observed line energy differences cannot be offered as any sort of confirmation of the author's proposal.

At least two immediately obvious objections can be offered to the proposed scheme. First, if the Wulf bands arise from an excited state, why does the transition present itself in a single band series? In particular, a ν_1'' series of the lower $\tilde{A}\,^1B_1$ state should be observed. Under the conditions of this experiment, it is doubtful that ozone in the $\tilde{A}\,^1B_1$ state exists in appreciable quantities for $\nu_1 > 2$ because of the short wavelength cutoff of

the White cell mirrors in addition to the natural decrease in band intensities observed in the $\tilde{A}\,^1B_1 \leftarrow \tilde{X}\,^1A_1$ transition (Wulf[11]). But, more important, from Wulf's observations of $\tilde{A}\,^1B_1 \leftarrow \tilde{X}\,^1A_1$, one sees that transitions from different ν_1 levels of the $\tilde{A}\,^1B_1$ state would almost exactly overlap (i.e., $2\nu_2'(^1A_2) \approx \nu_1''(\tilde{A}\,^1B_1)$). The presence of apparently unoverlapped structure in the 0.992 micron band does not contradict this explanation because the Wulf bands die out rapidly for wavelengths longer than 0.992 microns. Such an overlapping for the higher members of the series might also explain the presence of Lefebvre's "additional lines" (see p. 14 and 11).

A second, and more serious objection to the proposed $^1A_2 \leftarrow \tilde{A}\,^1B_1$ transistion is the question of why the 0.992 micron band should show any structure at all. If the diffuseness of the Chappuis bands is real and is caused by a straightforward predissociation process, then accordingly no structure should be observed in the Wulf bands, if indeed there would be sufficient concentration of $O_3(\tilde{A}\,^1B_1)$ for the Wulf bands to be observed at all. The author has no ready answer to this question.

Fortunately, the proposal set forth here is easily tested by experiment. If the conclusions are correct then the intensity of the Wulf bands should be a function of the density of radiation of wavelength 6000-4500A. Hopefully this experiment can be carried out in the near future.

Acknowledgements

The author is greatly indepted to Dr. Richard M. Badger, who suggested the subject of this project and whose advice, concern, and patiently shared knowledge were essential for the project's successful completion. The author also wishes to thank Dr. Oliver R. Wulf and Dr. George W. Robinson for their interest and advice.

Appendix

Abstract: An order of magnitude calculation shows that the predicted intensity of the proposed $^1A_2 \leftarrow A\,^1B_1$ transition is about 10^7 times weaker than the observed intensity of the Wulf bands. Hence the proposal set forth is quite obviously wrong. In view of these calculations, there can be little question that only transitions from the ground state are observable under the present experimental conditions.

It is suggested that the Wulf bands instead arise from a $^1A_2 \leftarrow X\,^1A_1$ transition, though molecular orbital calculations cast doubt on this assignment.

From the structure observed in the 0.922 micron band, the apex angle in the excited state is calculated to be 101.5°.

The appearance of structure at the red end of the series indicates that the principal dissociation products of $O_3(X\,^1A_1)$ are $O_2(^3\Sigma_g^-)$ with one quantum of vibrational excitation and $O(^3P)$.

Assuming that the Wulf bands do arise from the $^1A_2 \leftarrow A\,^1B_1$ transition proposed in the foregoing paper, it is possible to make an order of magnitude calculation of the expected band series intensity. Since the experimental conditions in Dr. Wulf's study are more ameniable to such a calculation than those in the present study, his data will be used.

Dr. Wulf employed a carbon arc source which drew about 8.5 amperes at 120 volts AC. Twelve inches from the arc a convex lens was used to create a parallel beam of light which was directed down the absorption column.*

Approximately 40 lumens/arc watt is propogated by a carbon arc under these conditions.[24] Thus the total radiant power is

$$P = 1000 \text{ watts} \times 40 \text{ lumens/watt} = 4 \times 10^4 \text{ lumens} = 6 \times 10^8 \text{ ergs/sec}.$$

Assuming that the arc is a blackbody radiator and that the arc temperature is 3500 °K, the energy density per cm^{-1} at 16,600 cm^{-1} (E_{vert} for $A\,^1B_1 \leftarrow X\,^1A_1$) "within" the arc is

$$\rho_{int}(16{,}600\,cm^{-1}) = 8\pi hc\nu^3 e^{-h\nu c/kT} = 2.5 \times 10^{-5} \text{ ergs/cm}^3\text{-cm}^{-1}.$$

From the "fourth power law", the effective radiative area of the arc is cal-

---

*From personal conversation with Dr. Wulf.

culated to be $A = \frac{P}{\sigma T^4} = 0.07\ cm^2$.

Assuming the surface of the arc to be spherical, the energy density/cm^{-1} at 16,600 cm^{-1} at the lens is

$$\rho_{lens}(16,600\ cm^{-1}) = \rho_{int.} \frac{0.07\ cm^2}{4\pi \times (2.54 \times 12)^2\ cm^2} = 1.5 \times 10^{-10}\ ergs/cm^3\text{-}cm^{-1}.$$

Due to reflection losses at the sides of the column, the average energy density within the column is approximately one-third of that at the lens. Therefore $\rho_{eff}(16,600\ cm^{-1}) = 5 \times 10^{-11}\ ergs/cm^3\text{-}cm^{-1}$.

From the observed oscillator strength of 6×10^{-5} for the Chappuis bands, one calculates that

$$B_{mn} = \frac{\pi e^2}{mhc^2\nu} f^{nm} = 4.8 \times 10^5\ cm^3 cm^{-1}/ergs\text{-}sec,$$

where B_{mn} is the usual electronic transition probability. If n is the number of molecules/cm^3 in the groundstate $\underline{X}\,^1A_1$, then the number of molecules/cm^3-sec undergoing the transition $\underline{A}\,^1B_1 \leftarrow \underline{X}\,^1A_1$ is

$$n B_{mn} \rho(16,600\ cm^{-1}).$$

By far the most important cause of the reverse transition is collision-induced emission. Approximate calculations give the result that each ozone molecule undergoes 4×10^8 collisions/sec. Assuming that one out of every four collisions involving $O_3(\underline{A}\,^1B_1)$ causes emission back to the ground state, the number of molecules/cm^3-sec undergoing $\underline{A}\,^1B_1 \rightarrow \underline{X}\,^1A_1$ is $n^* \times 10^8\ sec^{-1}$ where n^* is the average number of excited molecules/cm^3.

At equilibrium, we must have

$$n^* \times 10^8\ sec^{-1} = n B_{mn} \rho(16,600\ cm^{-1}),$$

or $$n^* = n B_{mn} \rho \times 10^{-8}\ sec = 1.8 \times 10^5\ cm^{-3}.$$

If we assume that the oscillator strength f'^{nm} of the proposed $^1A_2 \leftarrow \underline{A}\,^1B_1$ transition is 1, then

$$\int \kappa_\nu d\nu = n^* \frac{\pi e^2}{mc^2} f'^{nm} = 1.6 \times 10^{-7}\ cm^{-2},$$

where $\int \kappa_\nu d\nu$ is the integral of the extinction coefficient across the entire Wulf band series. From the present study, the experimental value for this integral is roughly 4 cm^{-2}. In view of the very large difference in magnitude between the calculated and observed integrals, there is little ques-

tion that the Wulf bands cannot be attributed to the proposed $^1A_2 \leftarrow \underline{A}\ ^1B_1$ transition. Similar considerations for other transitions show that only transitions from the ground state are at all likely to be observed.

If, indeed, the Wulf bands are due to ozone, seemingly the only remaining singlet-singlet transition which might be assigned is $K(18)(1a_2)^2(4a_1)^2(3b_2)(2b_1);\ ^1A_2 \leftarrow K(18)(1a_2)^2(4a_1)^2(3b_2)^2;\ \underline{X}\ ^1A_1$. This transition is predicted to be very weak since it is forbidden. In addition, the Walsh diagram suggests that the apex angle would undergo a decrease. On the other hand, the orbital energies implied by the above assignment are at considerable variance with those theoretically calculated.[16] It seems unlikely, in any case, that the Wulf bands arise from $\underline{a}^3B_1 \leftarrow \underline{X}\ ^1A_1$, as suggested by Robinson[13], since the apex angle undergoes a rather large decrease rather than an increase.

By use of the ground state parameters and the quadratic term constant in Eq.(3), the apex angle of the excited molecule is calculated to be 101.5°.

The sudden appearance of structure at the red end of the band series indicates that the dissociation energy of ozone lies between 9600 and 10,000 cm^{-1}. From thermodynamic data on the reaction $O_3(\underline{X}\ ^1A_1) \rightarrow O_2(^3\Sigma_g^-) + O(^3P)$, dissociation is calculated to be possible for energies greater than 8600 cm^{-1}. Since ω_e for $O_2(\quad)$ is 1580 cm^{-1}, we can conclude that the main dissociation products of $O_3(\underline{X}\ ^1A_1)$ are very likely $O_2(^3\Sigma_g^-)$ with one quantum of vibrational excitation and $O(^3P)$.

Table I: Vibrational Bands of Ground State Ozone

ν(obs)	ν(calc)	Assignmt. $v_1 v_2 v_3$	Peak Extinction α(cm^{-1};base 10)	Source
700.8 cm^{-1}		0 1 0	0.08	Gora[3]
1042.2*		0 0 1	6.0	KMN[4]
1113*		1 0 0	0.05	Estimate from VMNS[21]
1740	1726.3	0 1 1	0.04	HPS[22]
2111	2110.4	1 0 1	0.13	VMNS[21]
2786	2783.9	1 1 1	0.005	"
3046.4*		0 0 3	0.015	"
3698.5?[a]	3697.2	0 1 3	0.0036	This study
3847.4?[a]	3843.2	2 1 1	0.0012	"
4025.0*		1 0 3	0.012	"
4146.7*		1 3 1	0.00009	"
4254.4	4251.8	3 0 1	0.00028	"
4353.1*		0 2 3	0.00021	"
4505.7[b]	4511.4	2 2 1	0.00006	"
4517.2[b]	4514.8	0 5 1	0.00007	"
4665.2*		1 1 3	0.0010	"
4904.2*		3 1 1	0.00031	"
4924.6	4943.0	0 0 5	0.00052	"

Vibrational Energy Constants:

$\omega_1 = 1139.02$ cm^{-1} $\quad \chi_{11} = +0.84$ cm^{-1} $\quad \chi_{12} = -10.59$ cm^{-1}

$\omega_2 = 709.24$ $\quad \chi_{22} = +2.60$ $\quad \chi_{23} = -16.68$

$\omega_3 = 1099.68$ $\quad \chi_{33} = -13.37$ $\quad \chi_{13} = -44.80$

$$G(0,0,0) = 1453.45 \text{ cm}^{-1}$$

[a] Badly obscured by water vapor lines.
[b] These two levels are almost certainly perturbed.

Table II: Selection Rules for Electronic Transitions of Ozone

Species of Wavefunction Product $\psi_{el}' \psi_{el}''$	Predicted Relative Intensity	Polarization	Band Type
A_1	Medium	z	$\perp$
A_2	Forbidden	—	—
B_1	Weak	x	$\perp$
B_2	Strong	y	$\parallel$

Table III: Observed Electronic Spectra of Ozone and Assignments by Mulliken[16]

E_{vert}[23]	λ_{vert}	Rel. Int.[23]	Name	Orbital Trans.	State Trans.
1.55ev	8000A	?	Wulf bands		
2.04	6050	4	Chappuis	$2b_1 \leftarrow 4a_1$	$\underline{A}\,^1B_1 \leftarrow \underline{X}\,^1A_1$
3.58*	3440	1	Chalonge-Lefebvre		
3.95*	3135	50	Huggins		
4.85*	2550	8000	Hartley	$2b_1 \leftarrow 1a_2$	$\underline{B}\,^1B_2 \leftarrow \underline{X}\,^1A_1$

*There is some question as to whether these are all separate systems.

Table IV: Data on the Wulf Bands

Band No.	λ_{max}	$\lambda_{max(ave)}$	$\nu_{max(obs)}$	$\nu_{max(calc)}$	Peak Extinction $\alpha(cm^{-1}$, base 10)	Resolution
0	1.047, 8_5 μ	1.0478 μ	9544 cm^{-1}	9528 cm^{-1}	$0.03? \times 10^{-3}$	14 cm^{-1}
1	0.993, 3, 2, 2	0.9925	10076	10065	0.20×10^{-3}	15.5
2	0.944, 4_5, 3, 4, 4_5, 4	0.9940	10593	10606	0.25	15.5
3	0.896_5, 6, 8, 7_5	0.8970	11148	11153	0.31	8
4	0.851_5, 2, 5, 4, 4	0.8533	11719	11705	0.70	14
5	0.815, 6, 7_5, 7	0.8164	12249	12263	1.25	14
6	0.778_5, 8, 9_5, 8_0	0.7790	12837	12826	1.02	14
7	0.746_5, 7, 7_5, 8	0.7473	13382	13394	0.92	14
8	0.717, 6	0.7165	13957	13967	0.58	20
9	0.685, 4, 7, 6	0.6655	14588	14536	0.46/?	20
10	0.662, 2, 2, 2,	0.6620	15106	15130	0.30 ?	24

Least Square Curve:

$$\nu(cm^{-1}) = 9528.4 + 53361\,x + 2.654\,x^2$$

$$x = 0, 1, \ldots, 10$$

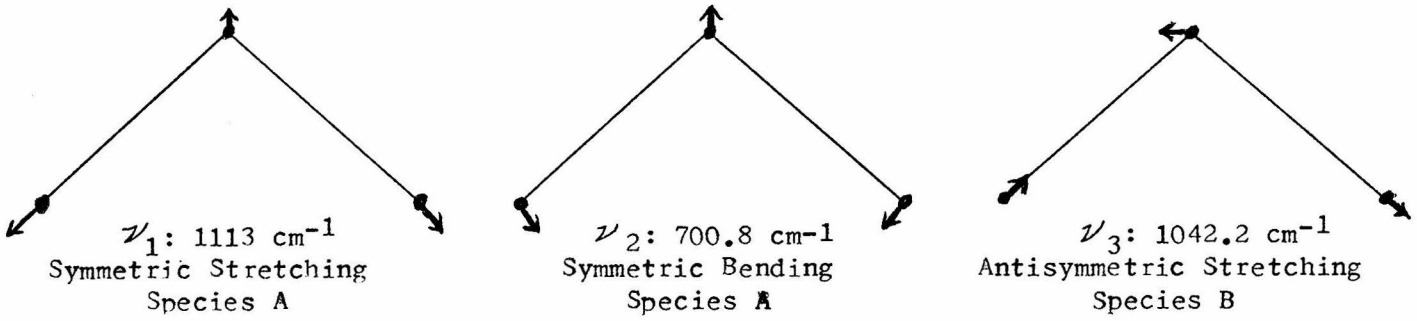

FIGURE I: The normal vibrations for a non-linear symmetrical X-Y-X molecule. Note that while the form of the antisymmetric stretching is completely determined by symmetry, the exact forms of ν_1 and ν_2 are dependent on the particular intermolecular forces involved; i. e., ν_1 and ν_2 may not involve "pure" stretching and bending respectively. For ozone the above forms are very nearly correct.

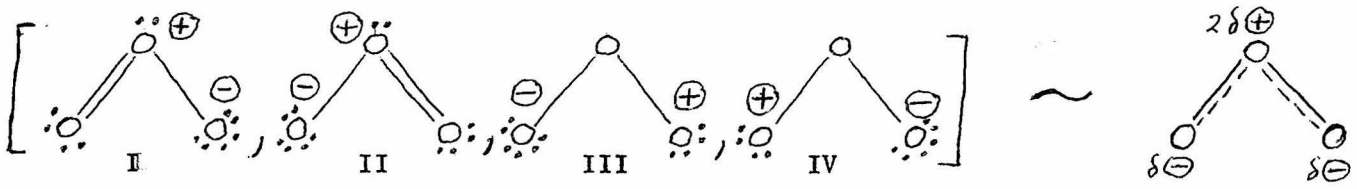

FIGURE II: The most probable resonance structures contributing to the ground electronic state of ozone. I and II are likely more important than III and IV because the former involve less charge separation.

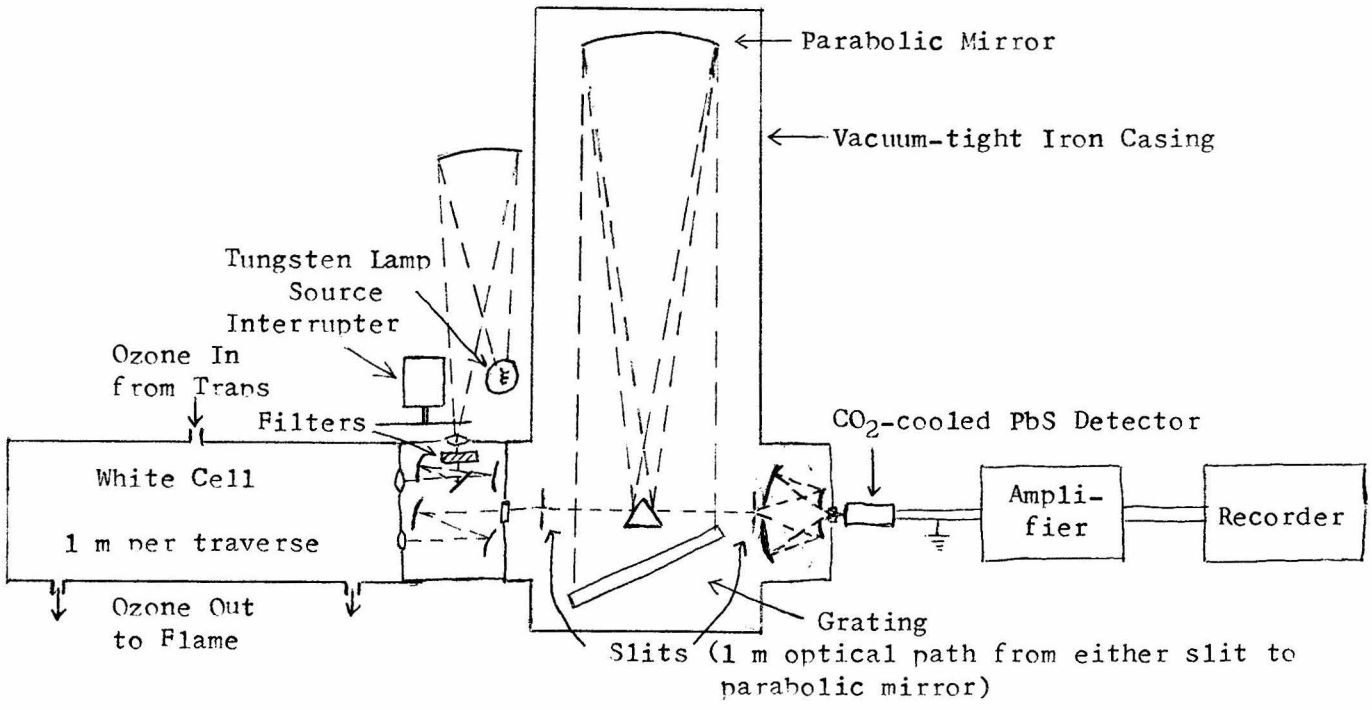

FIGURE III: Experimental Setup (not drawn to scale).

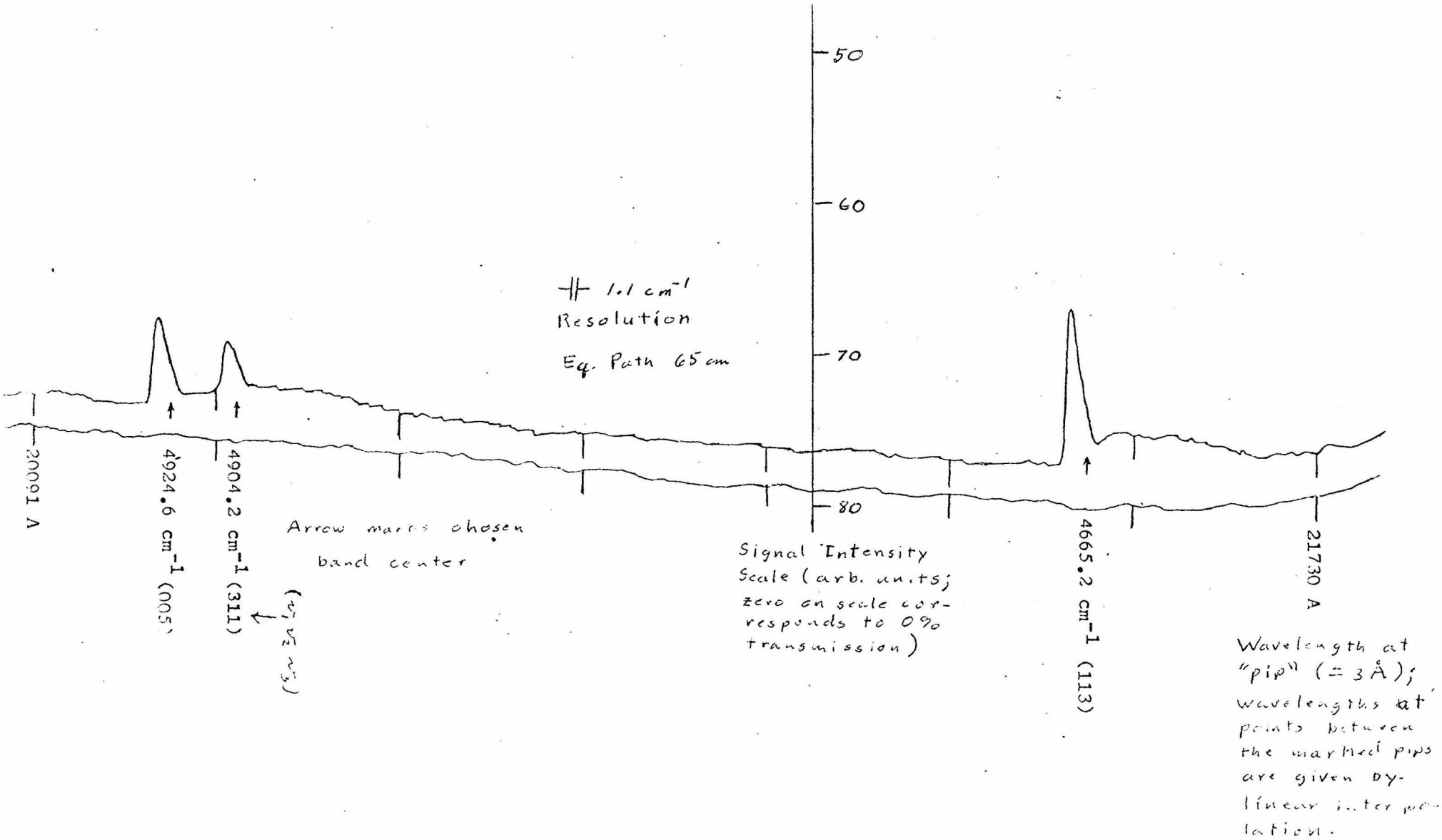
50
60
70
80
1.1 cm⁻¹ Resolution
Eq. Path 65 cm
20091 A
4924.6 cm⁻¹ (005)
4904.2 cm⁻¹ (311)
Arrow marks chosen band center
(ν1, ν2 ~ ν3)
Signal Intensity Scale (arb. units; zero on scale corresponds to 0% transmission)
4665.2 cm⁻¹ (113)
21730 A
Wavelength at "pip" (± 3 Å); wavelengths at points between the marked pips are given by linear interpolation.

FIGURE IV

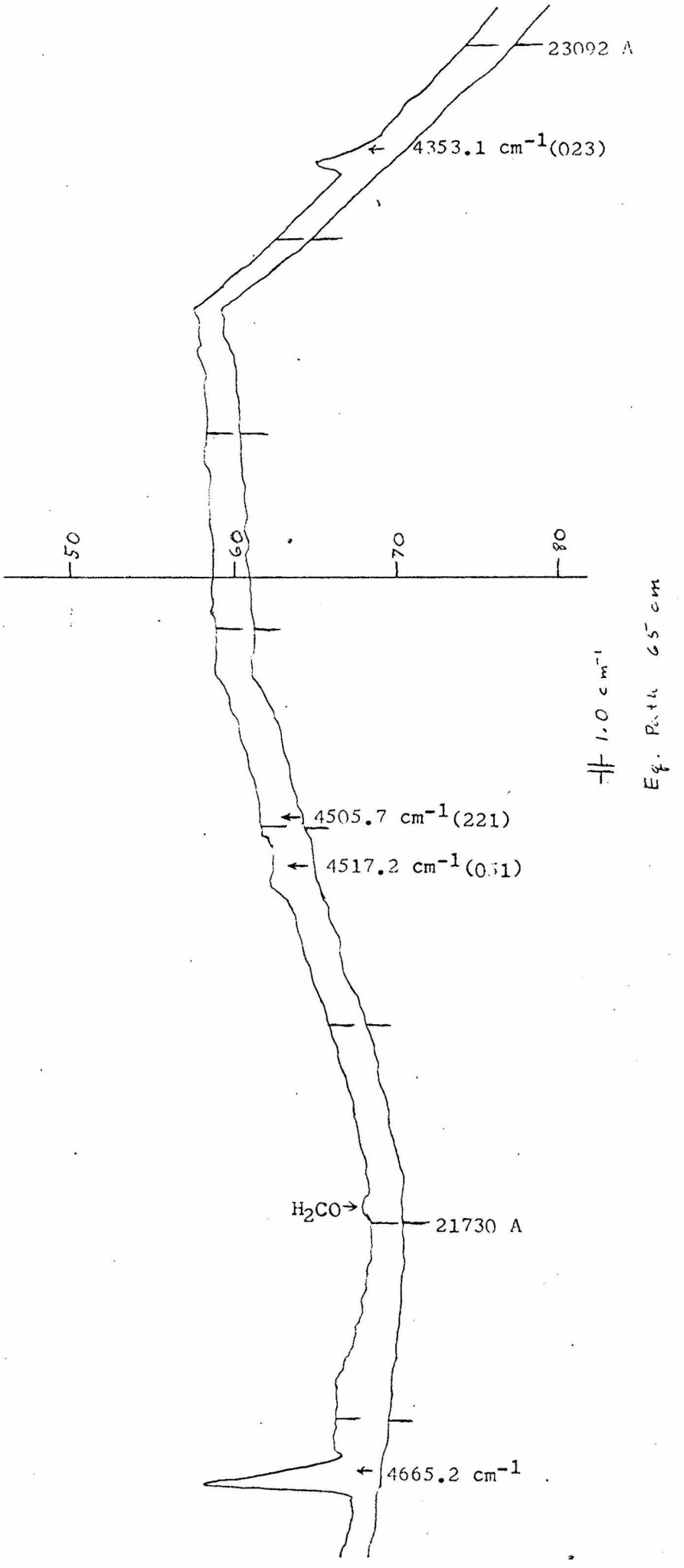

Figure XI (See Figure IX for experimental)

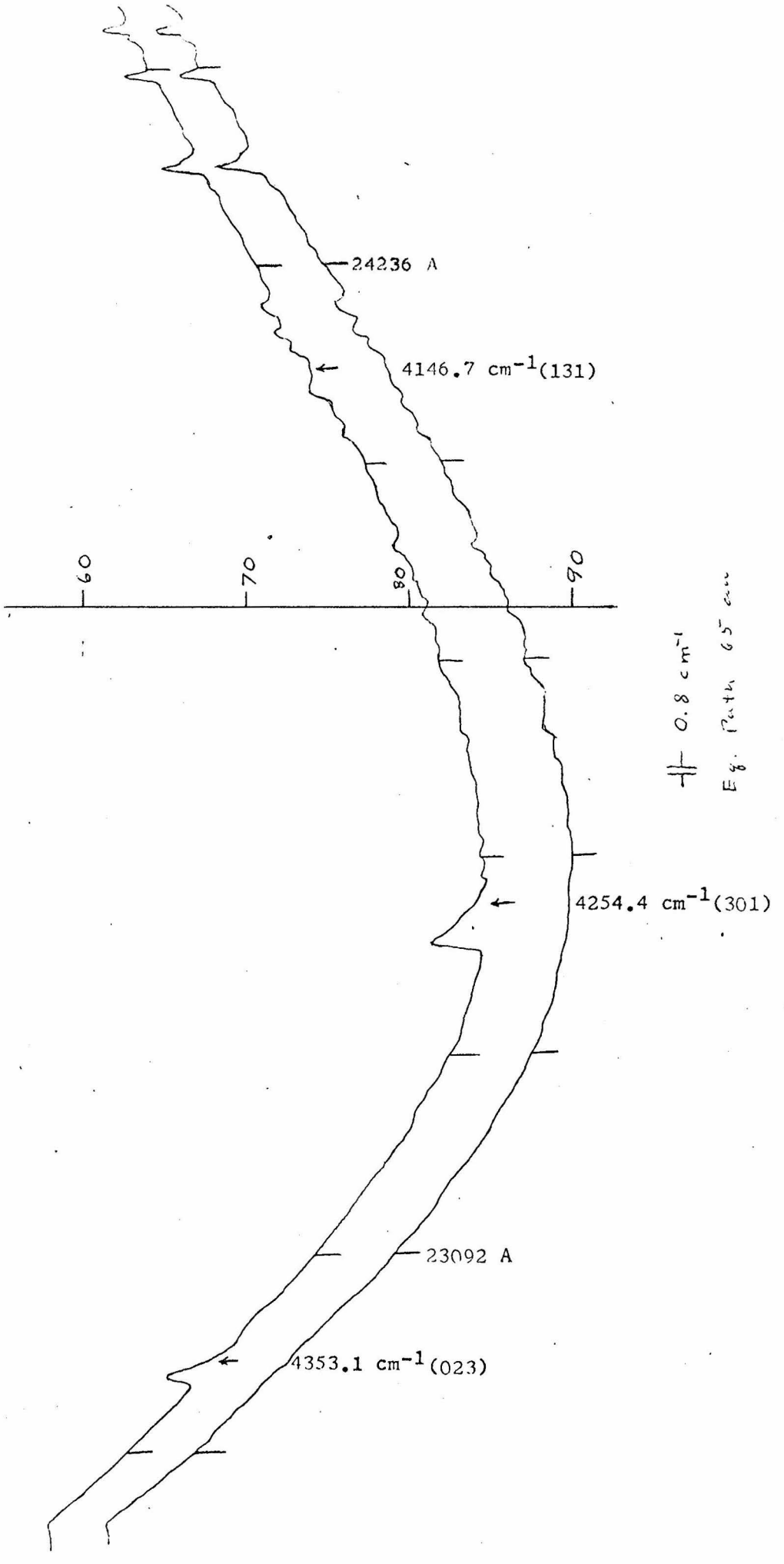
24236 A
4146.7 cm-1(131)
60
70
80
90
0.8 cm-1
Eff. Path 65 cm
4254.4 cm-1(301)
23092 A
4353.1 cm-1(023)

Figure VI

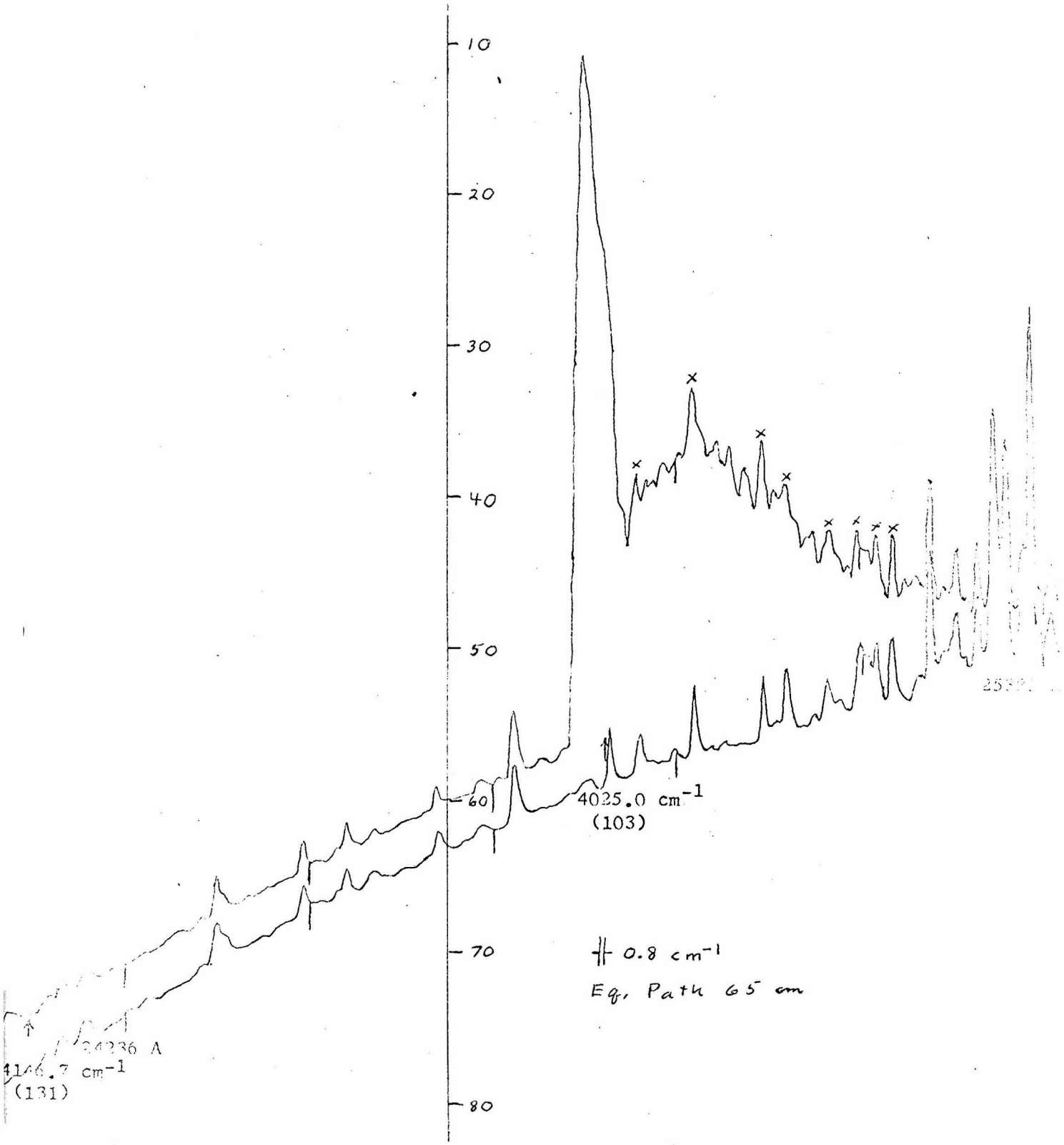
10
20
30
40
50
60
70
80
4025.0 cm-1
(103)
0.8 cm-1
Eq. Path 65 cm
24236 A
4146.7 cm-1
(131)

Figure VII

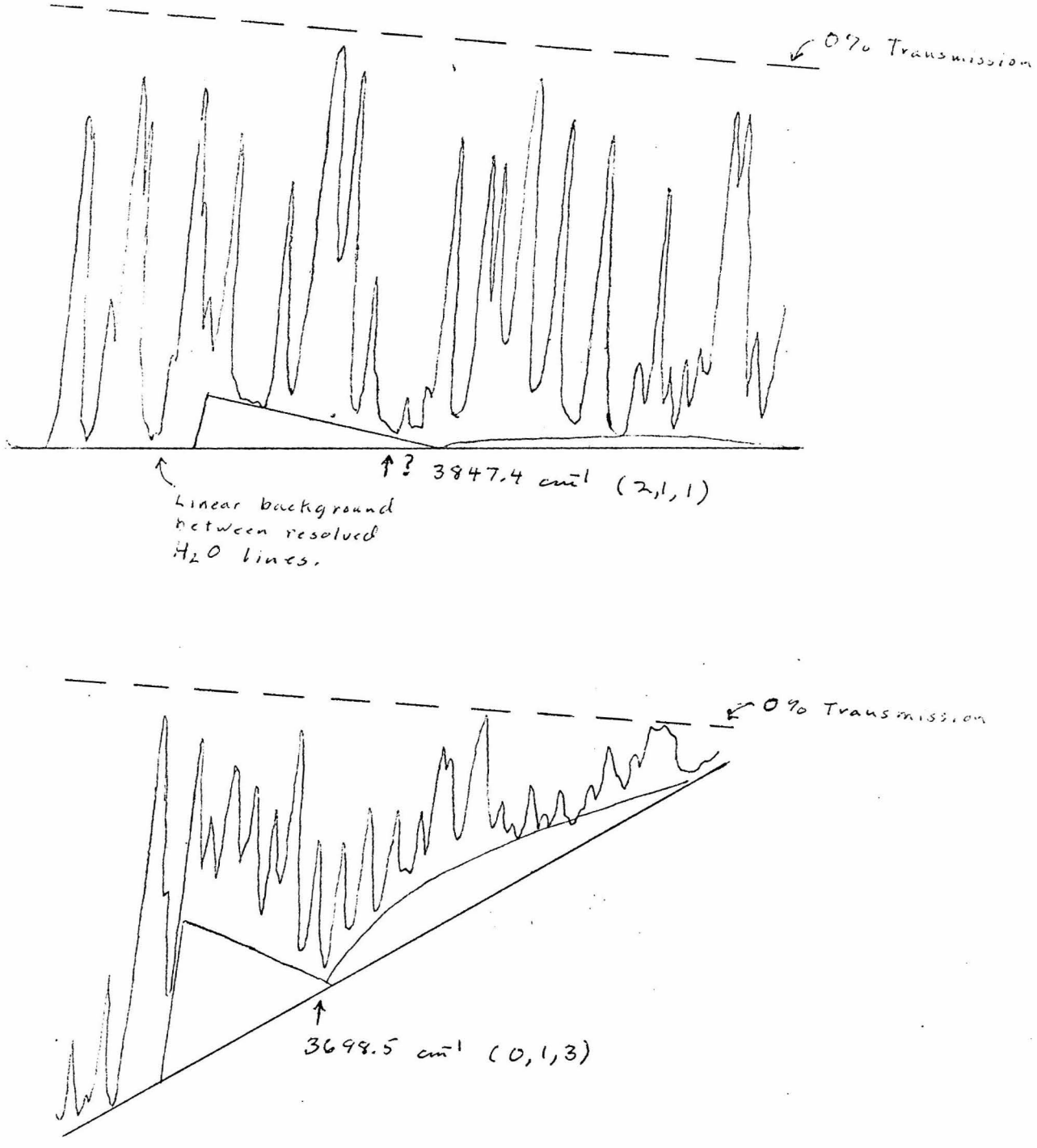
0% Transmission
? 3847.4 cm⁻¹ (2,1,1)
Linear background between resolved H_2O lines.
0% Transmission
3698.5 cm⁻¹ (0,1,3)

Figure VIII

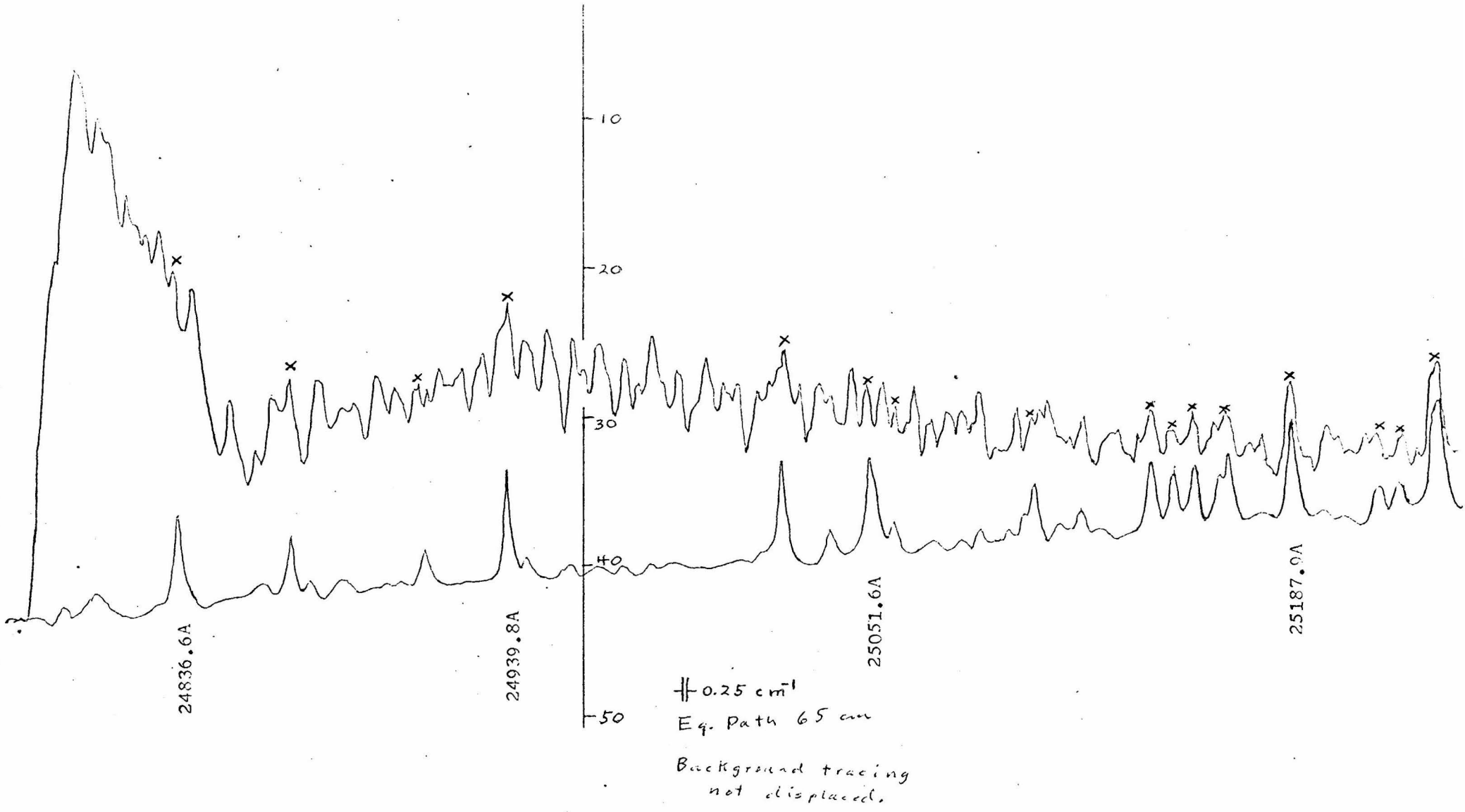
10
20
30
40
50
24836.6A
24939.8A
25051.6A
25187.9A
± 0.25 cm⁻¹
Eq. Path 65 cm
Background tracing
not displaced.

Figure IX

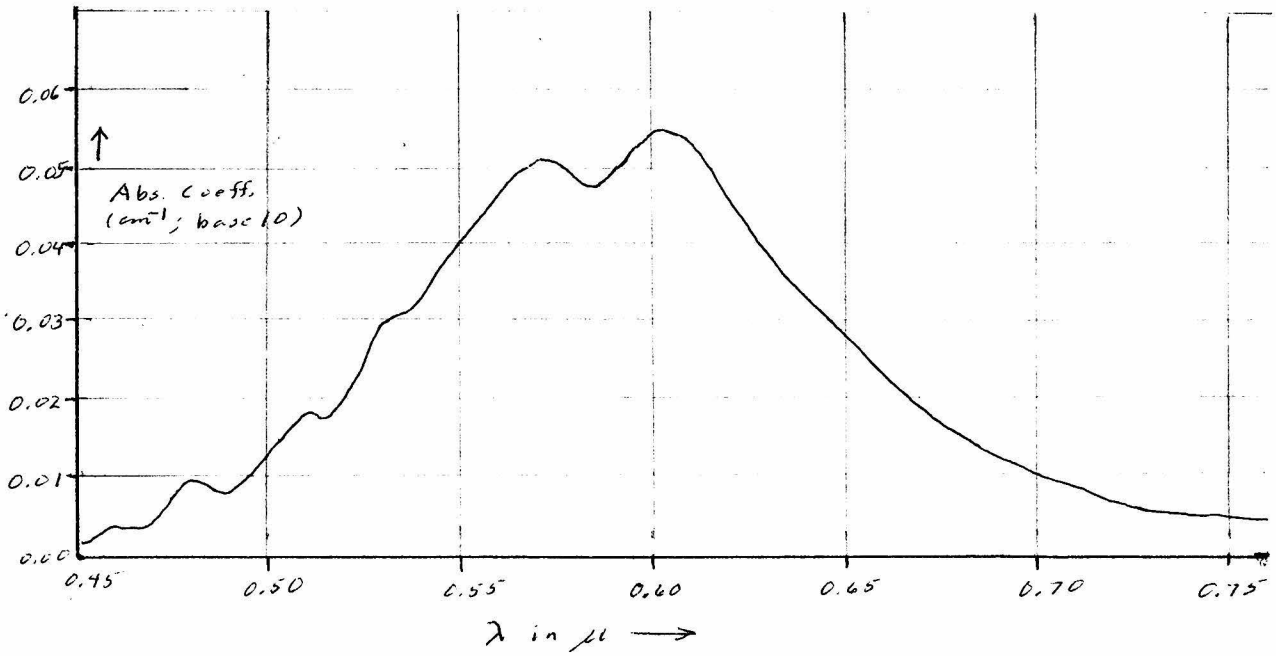

Figure X: The Chappuis Bands and Continuum of Ozone[18]

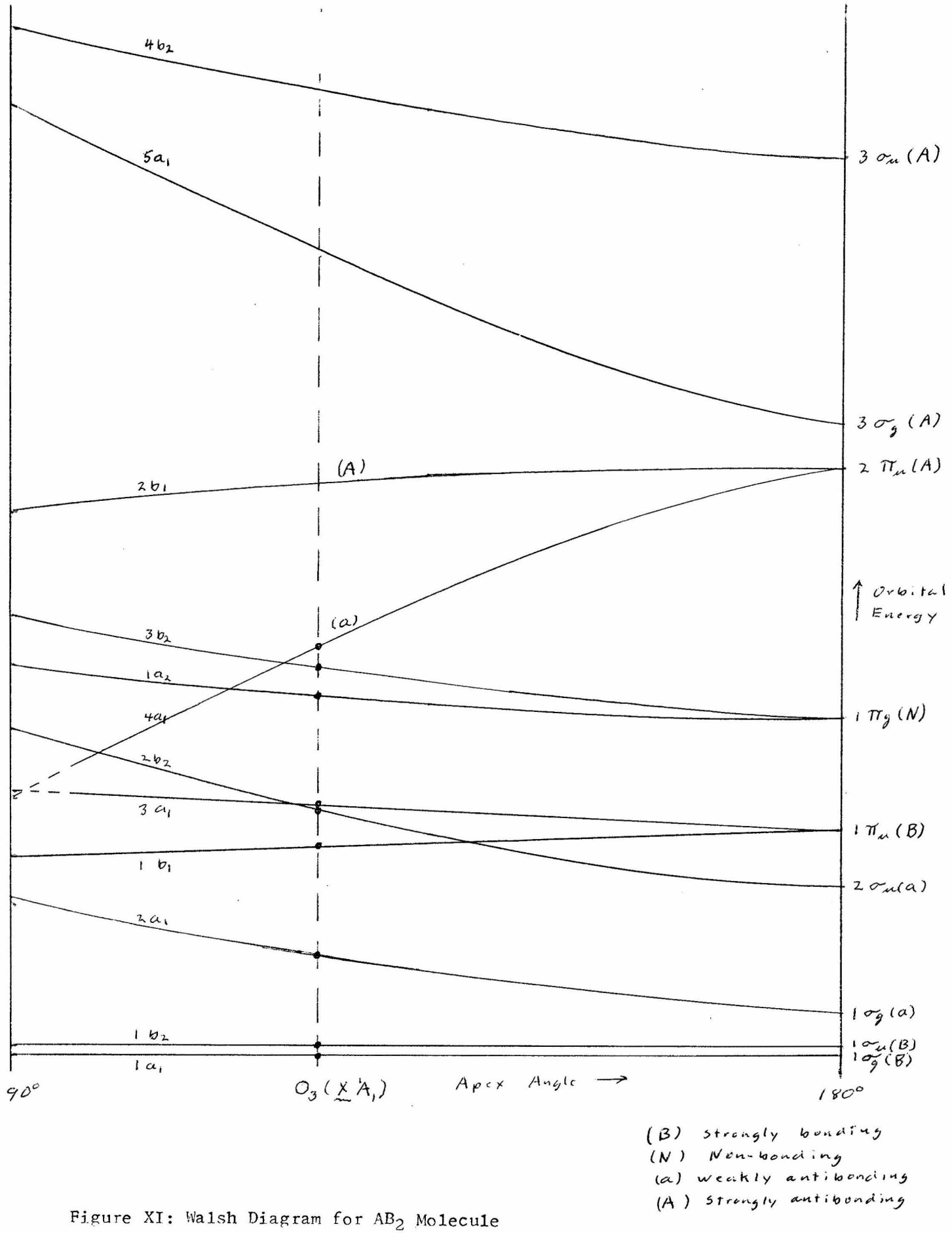

Figure XI: Walsh Diagram for AB_2 Molecule

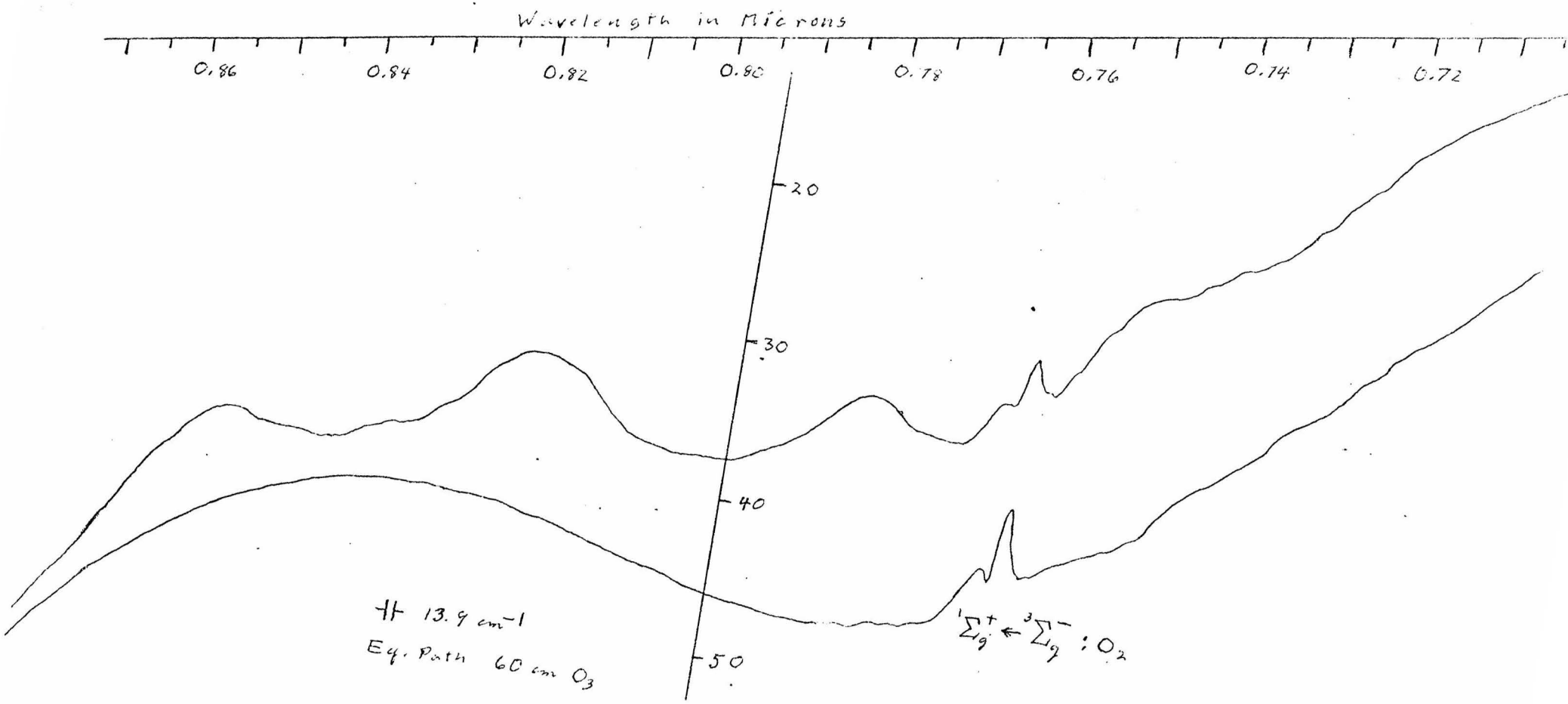

Figure II: The Strongest Wolf Band

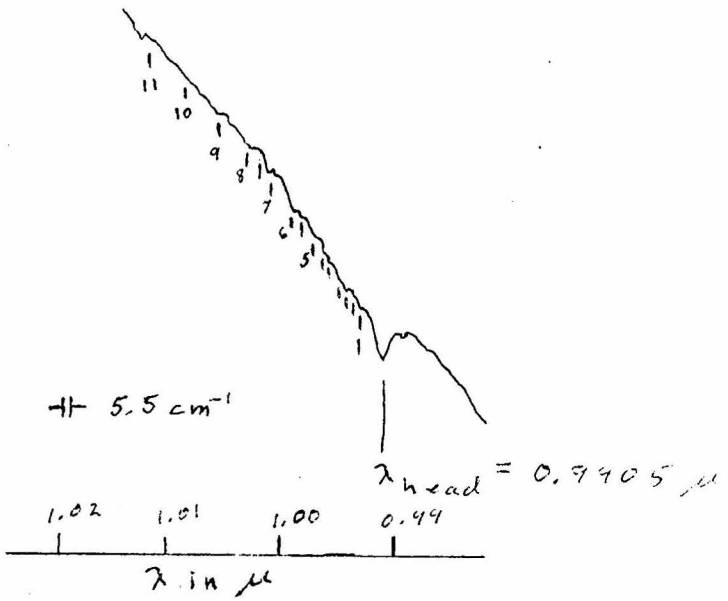

Figure XIII: The 0.992 Micron Band. Not all of the peaks noted are clearly visible in this single tracing.

Table of Reproducible Peaks (noted on at least four tracings out of six)

Peak No.	$\nu_{head} - \nu_{obs}$	$\nu_{head} - \nu_{calc}$
1	21.4 cm^{-1}	20.9 cm^{-1}
2	28.2	29.4
-	34.3	
3	42.0	40.2
4	53.3	53.5
-	57.9	
5	67.3	69.3
-	78.2	
6	87.2	87.5
7	105.0	108.0
-	117.9	
8	129.8	131.0
9	154.4	156.2
10	187.0	184.2
11	218.4	214.3

$$\nu_{calc}\,(cm^{-1}) = \nu_{head} - 10 - 1.210(x+2)^2$$

$$x = 1, 2, \ldots, 11$$

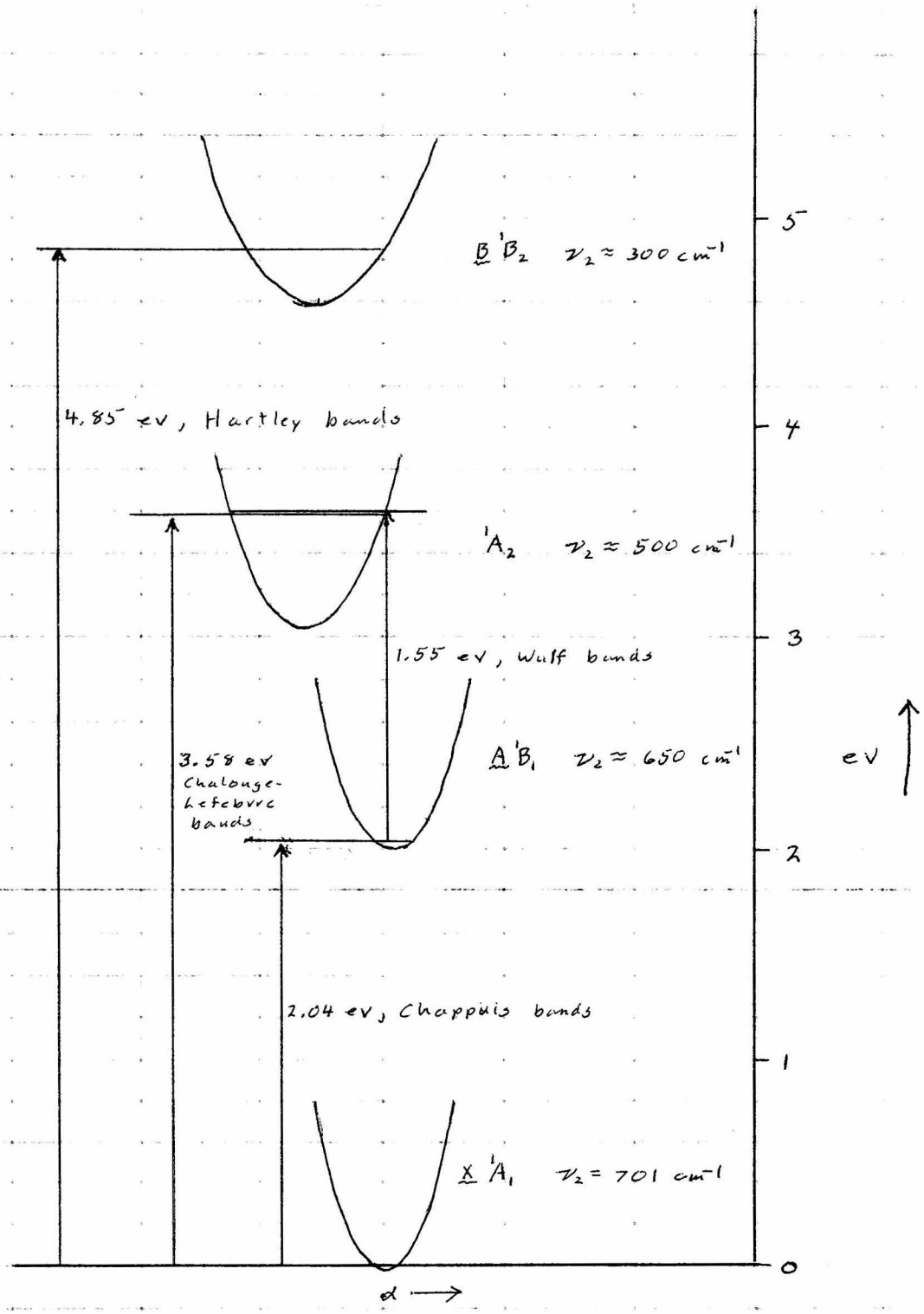

Figure XIV: The energies of the low-lying states of ozone. The ν_2 potential wells qualitatively show how the apex angle α is probably involved in each transition.

Footnotes

[1]G. Hettner, R. Pohlman, and H.J. Schumacher, Zeits. f. Physik 91, 372 (1934)

[2]M.K. Wilson and R.M. Badger, J. Chem. Phys. 16, 741 (1948)

[3]E.K. Gora, J. Mol. Spec. 3, 78 (1959)

[4]L. Kaplan, M. Migeotte, and L. Neven, J. Chem. Phys. 24, 1183 (1956)

[5]G.H. Herzberg, Molecular Spectra and Molecular Structure, Volume II, Van Nostrand Company, Inc., Princton, New Jersey, 1945

[6]R. Trambarulo, S.N. Ghosh, C.A. Burrus, Jr., and W. Gordy, J. Chem. Phys. 21, 851 (1953)

[7]E. O. Salant and W. West, Phys. Rev. 33, 640 (1929)

[8]R. Herman and L. Herman, Comp. rend. 230, 1516 (1950) report ground state interval of 1724cm^{-1} from uv emission. Their lines, however, do not seem to be in very good agreement with other sources.

[9]For earlier calculations, see F.F. Cleveland and M.J. Klein, J. Chem. Phys. 20, 337 (1952)

[10]See footnote[6]

[11]O.R. Wulf, Pr. Nat. Acad. Wash. 16, 507 (1930)

[12]L. Lefebvre, Comp. rend. 200, 1743 (1935)

[13]G.W. Robinson, contr., Methods of Experimental Physics, Volume III, Academic Press, New York, 1962, pp. 187-9, 214

[14]R.S. Mulliken, Rev. Mod. Phys. 14, 204 (1942)

[15]A.D. Walsh, J. Chem. Soc. (London) , 2260 (1953)

[16]R.S. Mulliken, Can. J. Chem. 36, 10 (1958)

[17]H. Sponer and E. Teller, Rev. Mod. Phys. 13, 75 (1941)

[18]Inn, Tanaka, J. Opt. Soc. Am. 43, 329, 870 (1953)

[19]N. Metropolis, Phys. Rev. 60, 283 (1941)

[20]D. Chalonge and L. Lefebvre Comp. rend. 197, 444 (1933)

[21]E. Vigroux, M. Migeotte, L. Neven, and J. Swensson, An Atlas of Nitrous Oxide, Methane and Ozone Infrared Absorption Bands, Institute for Astrophysics of the University of Liege; Technical Report, Phase B (part I) Contract AF61 (514)-432

[22]See footnote[1]

[23]L. Gmelin, Gmelins Handbuch der Anorganischen Chemie, Sauerstoff- Lieferung 4, Verlag Chemie, GMBH., Weinheim/Bergstrasse, 1960, pp. 1133-1139

[24]W.E. Forsythe, Smithsonian Physical Tables, Ninth Ed., Smithsonian Institution, Washington D.C., 1954, p. 105